

Lawrence Berkeley National Laboratory

Recent Work

Title

Isolation of a TMTAA-Based Radical in Uranium bis-TMTAA Complexes

Permalink

<https://escholarship.org/uc/item/2n8322p5>

Journal

Angewandte Chemie, 130(49)

ISSN

0044-8249

Authors

Hohloch, Stephan
Garner, Mary E
Booth, Corwin H
[et al.](#)

Publication Date

2018-12-03

DOI

10.1002/ange.201810971

Peer reviewed

Heavy and Guilty: Isolation of a TMTAA-Based Radical in Uranium bis-TMTAA Complexes

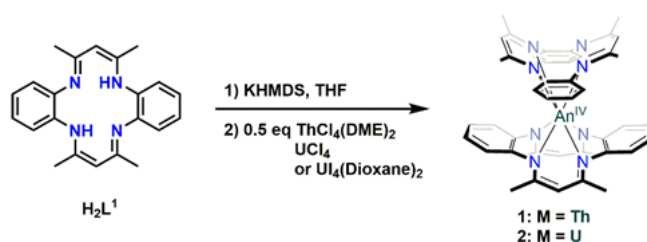
Stephan Hohloch,^{a,b,*†} Mary E. Garner,^{a†} Corwin H. Booth,^c Wayne W. Lukens,^c Colin A. Gould,^a Daniel J. Lussier,^{a,c} Laurent Maron,^{d,*} and John Arnold^{a,c,*}

Abstract: We report the synthesis, characterization, and electronic structure studies of a series of thorium(IV) and uranium(IV) bis-tetramethyltetraazaannulene complexes. These sandwich complexes show remarkable stability towards air and moisture, even at elevated temperatures. Electrochemical studies show the uranium complex to be stable in three different charge states; isolation of the oxidized species revealed a rare case of a non-innocent TMTAA ligand.

Coordination chemistry involving actinide elements has experienced a renaissance in recent years.^[1] Despite this surge in interest, the study of non-aqueous actinide chemistry is still relatively unexplored when compared to the s-, p-, and d-block metals, and lanthanides. Extensive oxidation state accessibility and potential for f-orbital participation make actinides promising candidates for small molecule activation,^[2] atom transfer reactions,^[3] hydrocarbon functionalization^[4] and magnetism.^[1g]

While these goals have been realized with organoactinide complexes containing the ubiquitous cyclopentadienyl “Cp” supporting ligand,^[5] the use of other ligands is still evolving.^[2,6] Macrocyclic ligands are promising alternatives because, like Cp, they provide the steric protection necessary to support large actinide ions. In fact, transition metal macrocycle complexes are well-known for their kinetic and thermodynamic stability due to the “macrocyclic effect”.^[7] Despite being widely explored with transition metals and lanthanides, surprisingly little is known about macrocyclic amine ligands in low-valent actinide chemistry; only a few porphyrin^[8] and phthalocyanine complexes^[9] and two corrole complexes,^[10] have been reported

so far. However, the synthesis of these macrocycles is often tedious involving multi-step synthetic and purification procedures, which are very time consuming and low yielding. An alternative macrocyclic ligand, which can be prepared in an easy three-step synthesis and on multi-gram scale is the tetramethyltetraazaannulene (TMTAA) ligand.^[11] This small-cored macrocyclic ligand has only been used twice in actinide chemistry - by us^[12a] and the Hayton group.^[12b,c] During our previous study we encountered a side reaction leading to the formation of the homoleptic sandwich complexes **1** and **2**. Herein we report the targeted synthesis of complexes **1** and **2** from readily available starting materials and describe their electronic and magnetic properties.



Scheme 1. Synthesis of complexes Th(TMTAA)₂ (**1**) and U(TMTAA)₂ (**2**)

Deprotonation of **H₂L** with 2 equiv of potassium hexamethyldisilazide (KHMDS) in THF followed by metalation with 0.5 equiv of ThCl₄(DME)₂, UCl₄(Dioxane)₂ or UCl₄ led to the formation of the corresponding homoleptic sandwich complexes **1** or **2** (Scheme 1). The yellow (**1**) and dark red (**2**) complexes displayed high solubility in THF, DME and chlorinated solvents, but moderate to low solubility in aromatic and aliphatic solvents, respectively. ¹H-NMR spectroscopy confirmed successful complexation as the resonance attributable to the backbone proton of the β-diketiminato subunit of the TMTAA ligands was shifted from 4.92 ppm in the free ligand (**H₂L**) to 4.26 ppm in **1** and 9.31 ppm in **2**. While chloroform solutions of **1** and **2** decomposed over the course of several days, benzene solutions showed remarkable stability: in fact, heating the complexes in benzene under air for several days did not lead to any signs of decomposition (see Figures S7 and S9).

The solid-state structures of the two complexes were determined by X-ray crystallography. Both complexes crystallized from THF/hexane mixtures (2:1) at -40°C. The complexes were found to be eight-coordinate with a square prismatic coordination environment (Fig. 1) wherein the two TMTAA ligands are rotated by about 90° to one another. Similar conformations have been seen for group IV^[13] and lanthanide^[14] bis-TMTAA complexes.

[a] Jun.-Prof. Dr. Stephan Hohloch, Mary E. Garner, Colin A. Gould, Daniel J. Lussier, Prof. Dr. John Arnold
Department of Chemistry
University of California, Berkeley
Berkeley, CA, 94720
E-Mail: Arnold@berkeley.edu

[b] Jun.-Prof. Dr. Stephan Hohloch
University of Paderborn
Warburger Straße 100
33098 Paderborn, Germany
E-Mail: Stephan.Hohloch@upb.de

[c] Dr. Corwin H. Booth, Dr. Wayne W. Lukens, Daniel J. Lussier, Prof. Dr. John Arnold
Chemical Science Division
Lawrence Berkeley National Laboratory
Berkeley, CA, 94720, United States

[d] Prof. Dr. Laurent Maron
LPCNO, Université de Toulouse, INSA Toulouse,
135 Avenue de Rangueil, 31077 Toulouse, France
E-Mail: laurent.maron@irsamc.ups-tlse.fr

† Both these authors contributed equally to this work.

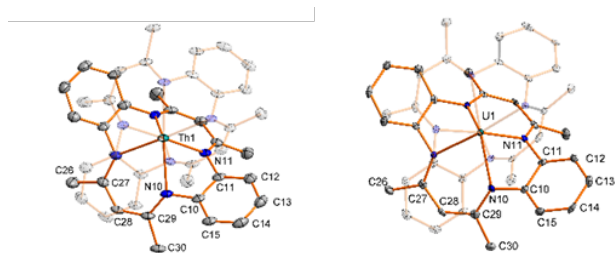


Figure 1. Molecular structure of **1**(left) and **2**(right). The “apical ligand” of the sandwich complexes are faded out for clarity. Hydrogen atoms, as well as additional solvents, have been omitted for clarity. Ellipsoids are shown at a probability level of 50 %.

The average An-N distances were found to be 2.491(3) Å in **1** and 2.449(4) Å in **2**. As a result of the small core size of the TMTAA ligand, the metals coordinate out-of-plane with respect to the nitrogen atoms of the two macrocycles. The metal was found to sit 1.559(1) Å above of the plane of TMTAA nitrogen atoms for **1** and 1.502(1) Å for **2**. Due to size of Th(IV), the out-of-plane coordination in **1** is the largest reported for a mononuclear TMTAA sandwich complex so far. Inspecting the space filling models of **1** and **2** (see Figure S21) identified the cause of the complexes’ pronounced stability towards air and moisture: in both, the actinide metal sits well-protected between the two staggered TMTAA ligands.

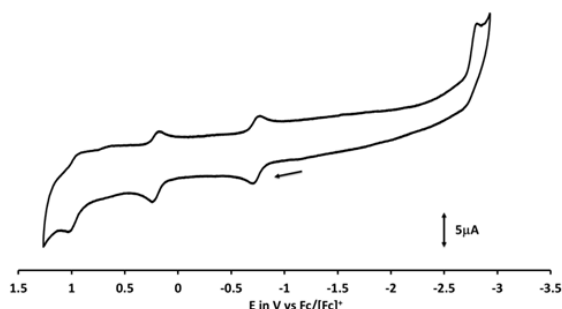
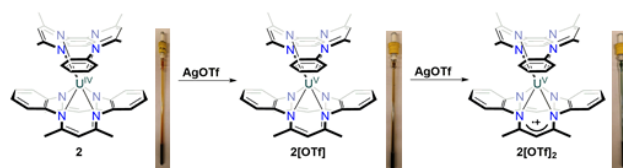


Figure 2. Cyclic voltammogram of **2** in 0.1 M NBu₄PF₆ vs Fc/Fc⁺ in MeCN. Scan rate 100 mV/s.

Next, we turned our attention to the electrochemical properties of the complexes. While the thorium complex **1** did not show any redox processes within the solvent window (1.2 V to -3 V; Figure S22), the uranium complex **2** exhibited two distinct and reversible oxidations at -0.73 V and 0.21 V vs ferrocene (see Figure S23). Considering the innocence of the thorium analogue (**1**), both processes observed for **2** were initially attributed to metal-centred oxidations corresponding to the uranium(IV/V) and uranium(V/VI) redox couples; DFT calculations (see supporting information for more details) also showed the SOMOs of **2** were located on the metal centre as expected for a uranium(IV) f^2 configuration (Figure 5, top).

Treatment of **2** with one equivalent of silver(I) triflate afforded the uranium(V) complex **2[OTf]** as a dark brown powder which was isolated in 75% yield (Scheme 2).



Scheme 2. Synthesis of the oxidized uranium bis TMTAA complexes **2[OTf]** and **2[OTf]₂** and their corresponding colours in solution

The ¹H NMR spectrum of **2[OTf]** suggested a successful oxidation, as all signals from the starting complex **2** were shifted. The resonance attributable to the TMTAA-CH proton, moved dramatically upfield from 9.35 ppm in **2** to -0.72 ppm in **2[OTf]**. In contrast to its U(IV) precursor (**2**), complex **2[OTf]** is not air stable and rapidly underwent decomposition when exposed to aerobic conditions. Structural investigations by single crystal X-ray diffraction revealed a shortening of the U-N bond distances in **2[OTf]** versus those of **2** by about 0.05 Å while the intra-ligand distances remained untouched (see Figure 4). Taken together, these data strongly indicated an oxidation of the uranium(IV) centre to uranium(V).

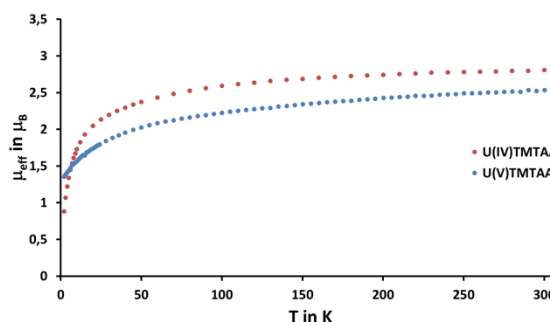
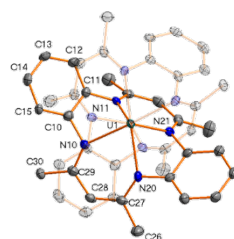


Figure 3. SQUID measurements on the complexes **2** (red) and **2[OTf]** (blue) plotted as T vs μ_{eff} .

Variable-temperature dc magnetic susceptibility data were collected for **2** and **2[OTf]** (see Figure 3). Complex **2** displays a room temperature μ_{eff} value of approximately 2.81 μ_{B} , similar to the value of 2.8 μ_{B} obtained via the Evans method; both of these values are lower than the U(IV) free-ion value of 3.58 μ_{B} , but fall well within the range reported for other U(IV) mononuclear complexes.^[15] The moment for **2** decreases with temperature, approaching a value of approximately 0.88 μ_{B} at 2 K, which is typical for a U(IV) ion possessing a poorly-isolated singlet ($M_J=0$) ground state arising from crystal field effects and its non-Kramers nature.^[1a,16] The magnetometry data for **2[OTf]** displays an expectedly smaller room temperature μ_{eff} than **2**, with a value of 2.54 μ_{B} , which is slightly higher than the Evans method measurement of 2.19 μ_{B} , but nearly matching the U(V) free-ion value of 2.54 μ_{B} , supporting the assignment of **2[OTf]** being a U(V) species.^[15] No EPR signal could be detected in the solid-state, even at 2 K, which is surprising since the S_4 symmetry of the U(V) site allows mixing between m_J substates with m_J differing by ± 4 . The resulting states, $a|7/2\rangle+b|-1/2\rangle$ and $c|5/2\rangle+d|-3/2\rangle$, where the number in the ket is m_J , are both EPR active. A weak EPR signal with $g = 3.3$ was detected in a frozen 0.01 M solution of **2[OTf]** in CH₂Cl₂ (Figure S25). The ground state magnetic moment of the species responsible for this signal is at least 1.6 μ_{B} . To better understand the EPR behaviour of **2[OTf]** silent, the χT curve obtained from the SQUID measurements

was extrapolated to 0 K (Figure S25) giving a ground state magnetic moment is $1.29 \mu_B$. This value is much smaller than that predicted by the EPR spectrum, which indicates that the EPR signal is likely due to a U(V) impurity rather than to **2[OTf]**. The χT curve of **2[OTf]** deviates from linearity above 8 K (compare Figure S24), which indicates that the first excited state is very low in energy, $10\text{-}15 \text{ cm}^{-1}$. The failure to observe an EPR spectrum for **2[OTf]** is likely due to very fast relaxation due to this low-lying state. To better understand the electronic structure of **2[OTf]**, computational studies were performed at the DFT level (see supporting information). Fixing the uranium to a +V oxidation state, the calculations reproduced experimental values of the X-ray structures well (see SI Table S3). Notably, the SOMO of **2[OTf]** (Figure 5, middle) displayed marked ligand character, which indicates that the unpaired electron is delocalized across the ligand and the metal centre.

Next, we attempted the double oxidation of **2** using 2.8 equiv of silver(I) triflate which afforded the teal-coloured complex **2[OTf]₂** in 75 % isolated yield. The compound was initially suspected to involve uranium(VI) due to the cyclic voltammetry data. However, NMR characterization of this new species revealed a paramagnetic compound with extensive broadening of the resonances. The resonances were distinctly shifted from those of either **2** or **2[OTf]** (see Figures S13 + S15). Single crystals suitable for X-ray diffraction studies were grown from a concentrated DCM solution at $-40 \text{ }^\circ\text{C}$. No conformational reorganization took place as a result of either single or double oxidation of **2**; the uranium centre is always in a square prismatic coordination environment. Analysis of the bond metrics of **2[OTf]₂** also indicated the oxidation occurred at a TMTAA ligand rather than at uranium centre. While the U-N distances do not change drastically (as would be expected for a metal-based oxidation), one of the C-N bond lengths within the ligand was found to be shortened, to $1.296(9) \text{ \AA}$. The fact that DFT calculations already suggested the non-innocent character of the TMTAA ligand in **2[OTf]**, the likelihood of a second oxidation at one of the TMTAA ligands, rather than the metal centre, could not be ruled out. Moreover, the uncommon teal colour of **2[OTf]₂** indicated an unusual electronic structure, as previously reported homoleptic uranium(VI) amide complexes are typically dark purple or black.^[18] To the best of our knowledge, there are no reports of structurally characterized stable radical TMTAA ligands. Instead, when oxidation or reductions are performed with TMTAA-containing molecules, follow up reactions at the ligand are typically observed (Scheme S1 and S2).^[19]



Distance	2	2[OTf]	2[OTf]₂
U1-N _{avg}	2.449(4) Å	2.396(5) Å	2.377(5) Å
U1-N _{1plane}	1.502(1) Å	1.461(1) Å	1.457(1) Å
C29-N10	1.334(4) Å	1.332(8) Å	1.296(9) Å

Figure 4. Structure of **2[OTf]₂** (left); Table compares the relevant bond distances of the three complexes. Further structural information can be found in the SI, Tables S1 and S2.

The UV-Vis spectrum of **2[OTf]₂** showed a diagnostic band at 580 nm that points towards ligand oxidation. In 2011, Wieghardt and Khusniyarov reported an oxidized β -diketiminato nickel complex of similar colour whose UV-Vis spectrum showed a similar band at 591 nm. The authors attributed the band to metal to ligand charge transfer (MLCT).^[21] Attempts to record the magnetic susceptibility of **2[OTf]₂** were unsuccessful. The sample is non-magnetic (neither paramagnetic nor diamagnetic) at low temperature due to cancellation of the inherent diamagnetism of the ligand by weak paramagnetism of the U centre. This result is consistent with a singlet ground state, either U(VI) and two TMTAA²⁻ ligands or U(V) strongly coupled to a ligand-based radical forming an open shell singlet in analogy to CoT_2Ce .^[20] Consistent with a singlet ground state, no EPR signal was observed for **2[OTf]₂** at 2 K. Since these spectroscopic methods did not unambiguously resolve the electronic structure of **2[OTf]₂**, we sought additional insight computationally.

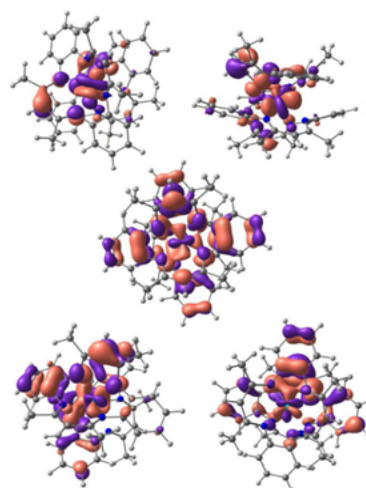


Figure 5. SOMOs of **2** (top), **2[OTf]** (middle) and **2[OTf]₂** (bottom).

Performing an energy optimization calculation on **2[OTf]₂** where the uranium oxidation state was fixed as +VI produced an optimized structure with U-N bond distances that were drastically different from those obtained experimentally through X-ray diffraction studies. In contrast, fixing the oxidation state of the uranium centre to +V and setting one TMTAA ligand to -1 (corresponding to an oxidized TMTAA mono-anion) reproduced the experimental bond metrics quite well (see Table S3). Analysis of the SOMOs of the complex revealed that the unpaired electron is not located on a single TMTAA, but is instead delocalized over both of the ligands, which also explains the chemical inertness of the complex (see Figure 5, top for the SOMOs). Additionally, TD-DFT calculation performed on **2[OTf]₂** suggested the band at 580 nm in the UV-Vis spectrum results from both a MLCT and a ligand to ligand charge transfer. Taken together, these data further support the second oxidation occurring at the TMTAA ligand (see SI Figure S26). To obtain further information on the electronic structure of this unique TMTAA radical, we performed CASSCF calculations wherein the two unpaired electrons were distributed across 4 orbitals (2 uranium f-orbitals and two π^* -orbitals of the ligand). We found

that the ground state was an open-shell triplet with the associated open-shell singlet configuration only 0.009 eV higher in energy, the closed-shell singlet (U(VI)) being 2.71 eV above the ground state. This is consistent with the inability to obtain useful SQUID or EPR data on this complex. We believe that the line broadening in the NMR results from the population of excited magnetic states at room temperature. In sum, these calculations, X-ray data, and UV-Vis data strongly indicate the electronic structure of **2**[OTf]₂ is best described as U(V)-TMTAA(1.5-)-TMTAA(1.5-) akin to the previously described multi-configurational cerocene, which also possess a singlet ground state.²⁰

In conclusion, we have presented the first air- and moisture-stable actinide(IV) bis-TMTAA sandwich complexes. The uranium complex **2** was found to undergo two reversible oxidations. The first oxidation is metal-centred, while the second oxidation leads to a unique example of an oxidized, non-innocent TMTAA ligand. Notably, **2**[OTf]₂ represents the first structurally characterized TMTAA complex, where the TMTAA ligand undergoes oxidation and no further chemical transformations.¹⁹ We believe that this exciting and unprecedented chemistry can be applied to transuranic metals including neptunium and we are interested in exploring the reactivity of the radical TMTAA complex **2**[OTf]₂ towards small molecules.

Acknowledgements

S.H. acknowledges the German Academic Exchange Service (DAAD) for a postdoctoral scholarship. M.E.G. acknowledges the NSF-GRFP (CHE-0840505) for a graduate research fellowship. This work was supported by the Director, Office of Science, Office of Basic Energy Sciences, Division of Chemical Sciences, Geosciences, and Biosciences Heavy Element Chemistry Program of the U.S. Department of Energy (DOE) at LBNL under Contract No. DE-AC02-05CH11231. We also acknowledge Prof. Dr. Jeff Long for the use of his SQUID magnetometer, supported by NSF grant CHE-1800252.

Keywords: TMTAA • uranium • thorium • macrocycles • non-innocence

- [1] a) C.J. Burns, M.S. Eisen, In "The Chemistry of the Actinide and Transactinide Elements; L.R. Morss, N.M. Edelstein, J. Fuge, Eds.; Springer: Berlin, Heidelberg, 2006; Vol. 5. b) T.W. Hayton, *Chem. Commun.*, 2013, **49**, 2956. c) M. Ephritikhine, *Organometallics*, **2013**, *32*, 2464. d) S.T. Liddle, *Angew. Chem. Int. Ed.*, **2015**, *54*, 8604. e) A.R. Fox, S.C. Bart, K. Meyer, C.C. Cummins, *Nature*, **2008**, *455*, 341. f) F. Moro, D.P. Mills, S.T. Liddle, J. van Slageren, *Angew. Chem Int. Ed.*, **2013**, *52*, 3430. g) S.T. Liddle, J. van Slageren, *Chem. Soc. Rev.*, **2015**, *44*, 6655.
- [2] I. Castro-Rodriguez, H. Nakai, L.N. Zakharov, A.L. Rheingold, K. Meyer, *Science*, **2004**, *305*, 1757.
- [3] W.J. Evans, S.A. Kozimor, J.W. Ziller, *Science*, **2005**, *309*, 1835.
- [4] E. Barnea, M. Eisen, *Coord. Chem. Rev.*, **2006**, *250*, 855.
- [5] a) L.T. Reynolds, G.J. Wilkinson, *J. Inorg. Nucl. Chem.*, **1956**, *2*, 246-253. b) *Organometallic and Coordination Chemistry of the Actinides*; T.E. Albrecht-Schmitt, Ed.; Springer: Berlin, Heidelberg, **2008**, Vol 127.
- [6] a) M.A. Boreen, B.F. Parker, T.D. Lohrey, J. Arnold, *J. Am. Chem. Soc.*, **2016**, *138*, 15865. b) B.M. Gardner, S.T. Liddle, *Chem. Commun.*, **2015**, *51*, 10589. c) C. Camp, N. Settineri, J.Lefèvre, A.R. Jupp, J. M. Goicoechea, L. Maron, J. Arnold, *Chem. Sci.*, **2015**, *6*, 6379. d) N. Settineri, M.E. Garner, J. Arnold, *J. Am. Chem. Soc.*, **2017**, *139*, 6261. e) M.E. Garner, S. Hohloch, L. Maron, J. Arnold, *Organometallics*, **2016**, *35*, 2915. f) M.E. Garner, S. Hohloch, L. Maron, J. Arnold. *Angew. Chem. Int. Ed.*, **2016**, *55*, 13789. g) M.E. Garner, J. Arnold, *Organometallics*, **2017**, *36*, 4511–4514. h) M.E. Garner, B.F. Parker, S. Hohloch, R.G. Bergman, J. Arnold, *J. Am. Chem. Soc.*, **2017**, *139*, 12935. i) S. Hohloch, J.R. Pankhurst, E.E. Jaekel, B.F. Parker, D.J. Lussier, M.E. Garner, C.H. Booth, J.B. Love, J. Arnold, *Dalton Trans.*, **2017**, *46*, 11615. j) M.E. Garner, T.D. Lohrey, S. Hohloch, J. Arnold, *J. Organomet. Chem.* **2018**, *857*, 10–15.
- [7] D.K. Cabbinness, D.W. Magerum, *J. Am. Chem. Soc.*, **1969**, *91*, 6540.
- [8] a) O. Bilsel, J. Rodriguez, D. Holten, G.S. Girolami, S.M. Milam, K.S. Suslick, *J. Am. Chem. Soc.*, **1990**, *112*, 4075. b) G.S. Girolami, S.N. Milam, K.S. Suslick, *Inorg. Chem.*, **1987**, *26*, 343. c) A. Dormond, B. Belkam, R. Guillard, *Polyhedron*, **1984**, *3*, 107.
- [9] a) K.M. Kadish, G. Moninot, Y. hu, D. Dubois, A. Ibnlfassi, J.M. Barbe, R. Guillard, *J. Am. Chem. Soc.*, **1993**, *115*, 8153. b) R. Guillard A. Dormond, M. Belkalem, J.E. Anderson, Y.H. Liu, K.M. Kadish, *Inorg. Chem.*, **1987**, *26*, 1410.
- [10] A.L. Ward, H.L. Buckley, W.W. Lukens, J. Arnold, *J. Am. Chem. Soc.*, **2013**, *135*, 13965.
- [11] a) P. Mountford, *Chem. Soc. Rev.*, **1998**, *27*, 105. b) F.A. Cotton, J. Czuchajowska, *Polyhedron*, **1990**, *9*, 1217. c) E.G. Jaeger, *Z. Allg. Anorg. Chem.*, **1969**, *177*. d) V.L. Goedken, J. Molin Case, Y.-A. Whang, *J. Chem. Soc., Chem. Commun.*, **1973**, 337.
- [12] a) S.Hohloch, M.E. Garner, B.F. Parker, J. Arnold, *Dalton Trans*, **2017**, *46*, 13768. b) E.A. Pedrick, M.K. Assefa, M.E. Wakefield, G. Wu, T.W. Hayton, *Inorg. Chem.*, **2017**, *56*, 6638. c) M.K. Assefa, E.A. Pedrick, M.E. Wakefield, G. Wu, T.W. Hayton, *Inorg. Chem.*, **2018**, *57*, 8317.
- [13] S. De Angelis, E. Solari, E. Gallo, C. Floriani, A.Chiesi-Villa, C. Rizzoli, *Inorg. Chem.*, **1992**, *31*, 2520.
- [14] a) U.J. Williams, B.D. Mahoney, P.T. DeGregorio, P.J. Caroll, E. Nakamuro-Ogiso, J.M. Kikkawa, E.J. Schelter, *Chem. Commun.*, **2012**, *48*, 5593. b) U.J. Williams, B.D. Mahoney, A.J. Lewis, P.T. DeGregorio, P.J. Carroll, E.J. Schelter, *Inorg. Chem.*, **2013**, *52*, 4142. c) M.D. Walter, R. Fandos, R.A. Anderson, *New J. Chem.*, **2006**, *30*, 1065.
- [15] D.R. Kindra, W.J. Evans, *Chem. Rev.*, **2014**, *114*, 8865.
- [16] a) B. Kanellakopoulos, *Organometallics of the f-Elements*, D. Reidel Pub. Co., Dordrecht, The Netherlands, **1978**; b) T. H. Siddall, *Theory and Applications of Molecular Paramagnetism*, Wiley, New York, **1976**.
- [17] Abragam, A.; Bleaney, B. *Electron Paramagnetic Resonance of Transition Ions*. Clarendon Press. Oxford. **1970**
- [18] a) L.A. Seaman, S. Fortier, G. Wu, T. Hayton, *Inorg. Chem.*, **2011**, *50*, 636. b) K. Meyer, D.J. Mindiola, T.A. Baker, W.M. Davis, C.C. Cummins, *Angew. Chem. Int. Ed.*, **2000**, *39*, 3063.
- [19] V.L. Goedken, J.A. Ladd, *J. Chem. Soc., Chem. Commun.*, **1981**, 910
- [20] a) M. Dolg, P. Fulde, W. Kuechle, C.S. Neumann, H. Stoll, *J. Chem. Phys.*, **1991**, *94*, 3011. b) M. Dolg, P. Fulde, H. Stoll, H. Preuss, A. Chang, R.M. Pitzer, *Chem. Phys.*, **1995**, *195*, 71. c) M.D. Walter, C.H. Booth, W.W. Lukens, R.A. Anderson, *Organometallics*, **2009**, *28*, 698. d) A. Kerridge, R. Coates, N. Kaltsoyannis, *J. Phys. Chem. A.*, **2009**, *113*, 2896. e) C.-S. Neumann, P. Fulde, *Z. Physik B.* **1989**, *74*, 277. f) C.H. Booth, M. Walter, M. Daniel, W.W. Lukens, R.A. Andersen, *Phys. Rev. Lett.*, **2005**, *95*, 267202.
- [21] a) M.M.Khusniyarov, E. Bill, T. Weyhermüller, E. Bothe, K. Wieghardt, *Angew. Chem. Int. Ed.*, **2011**, *50*, 1652. b) C. Camp, J. Arnold, *Dalton Trans.*, **2016**, *45*, 14462.